

Future climate change impacts on runoff of scarcely gauged Jhelum river basin using SDSM and RCPs

Saira Munawar ^{a,b}, Muhammad Naveed Tahir^{b,c,*} and Muhammad Hassan Ali Baig^b

^a Department of Geography, University of Gujrat, Gujrat, Pakistan

^b Institute of Geo-information & Earth Observation, Pir Mehr Ali Shah Arid Agriculture University, Rawalpindi, Pakistan

^c Department of Agronomy, Pir Mehr Ali Shah Arid Agriculture University, Rawalpindi, Pakistan

*Corresponding author. E-mail: naveed@uaar.edu.pk

 SM, 0000-0002-8219-5088

ABSTRACT

Climate change is a global issue and causes great uncertainties in runoff and streamflow projections, especially in high-altitude basins. The quantification of climatic indicators remains a tedious job for the scarcely gauged mountainous basin. This study investigated climate change by incorporating GCM (CCSM4) using the SDSM method for RCPs in the Jhelum river basin. Historical climatic data were coupled with Aphrodite data to cope with the scarcity of weather stations. SDSM was calibrated for the period 1976–2005 and validated for the period 2006–2015 using R^2 and RMSE. Future climatic indicators were downscaled and debiased using the MB-BC method. The de-biased downscaled data and MODIS data were used to simulate discharge of Jhelum river basin using SRM. Simulated discharge was compared with measured discharge by using Dv% and NSE. The R^2 and RMSE for SDSM range between 0.89–0.95 and 0.8–1.02 for temperature and 0.86–0.96 and 0.57–1.02 for precipitation. Projections depicted a rising trend of 1.5 °C to 3.8 °C in temperature, 2–7% in mean annual precipitation and 3.3–7.4% in discharge for 2100 as compared to the baseline period. Results depicted an increasing trend for climatic indicators and discharge due to climate change for the basin.

Key words: climate change, GCM, RCPs, SDSM, SRM

HIGHLIGHTS

- Climate change has great impacts on the hydrological cycle of the river basin.
- Statistical downscaling is the more efficient technique to project climate change using GCMs.
- Hydrology of the mountainous river basin has been severely impacted by temperature rise and glacier/snow melting.
- The climatic and hydrologic projections for the mountainous river Jhelum basin were made for two RCPs (RCP-4.5 and RCP-8.5).

INTRODUCTION

Climate change is one of the leading environmental issues of the 21st century and has impacts on the hydrological cycle (IPCC 2013). The Earth's temperature is rising continuously and triggering changes in fresh water supplies which ultimately affect agriculture. Pakistan is an agrarian economy and largely reliant on frozen water resources due to snow-covered mountain tops and glaciated ice that maintain the perennial water flows in the country's rivers. Himalayan glaciers are a huge concentration of ice exterior to the polar regions and feed the major river systems of South Asia. The water resources of Pakistan are significantly vulnerable to climate variability and climate change (Mahmood & Jia 2016).

Snowmelt runoff simulation in rugged mountainous regions is a complex process under changing climate due to its unique hydrological cycle mainly contributed by snowmelt, glacial melt water, and precipitation (Jin *et al.* 2019). The rise in global average temperature has a direct impact on precipitation because it drives evapotranspiration, therefore increasing water vapor concentration in the atmosphere (Mandal *et al.* 2016). The temperature rise also accelerates snow and ice melting, supplementing the runoff in the mountainous regions, and these snow-covered tops are the main fresh water source for the low lying stream areas. The major reservoirs of Pakistan are dependent on glacial meltwater runoff generated from the

This is an Open Access article distributed under the terms of the Creative Commons Attribution Licence (CC BY 4.0), which permits copying, adaptation and redistribution, provided the original work is properly cited (<http://creativecommons.org/licenses/by/4.0/>).

snow-covered area (SCA) of the Upper Indus Basin (UIB) for their water supply (Khairul *et al.* 2019). It is essential to monitor climate change impact assessment on hydrological cycles for water resource management and planning.

Global climate models (GCMs) provide useful quantitative information for future climatic changes at regional and global scales at coarse resolution (250–600 km) but their direct use is limited for future climate change projection at local level (Pervez & Henebry 2014). To cover the differences between GCMs' resolution and local variables at the observation levels, downscaling methods are used on corresponding models (Tahir *et al.* 2018). There are two downscaling methods, statistical downscaling and dynamic downscaling. Statistical downscaling is more preferred in situations where low cost and rapid assessment of climatic variables is required to predict climate trends at local level (Hasan *et al.* 2018). The statistical downscaling method (SDSM) facilitates the rapid development of low-cost, multiple, single-site scenarios of daily weather variables for current and future climate projections. Community Climate System Model version 4 (CCSM4) GCM data were selected for statistical downscaling and forecasting of future climatic change at the local level of Jhelum river basin under Representative Concentration Pathways (RCPs). RCPs are scenarios established on greenhouse gas emissions (GHGs) concentrations to assess the future climate change trends globally (Baek *et al.* 2013). RCPs were selected as standard scenarios for the IPCC Fifth Assessment Report. RCPs consider time paths for GHG emissions and concentrations for live climatic projections. This study considered one medium stabilization scenario, RCP4.5, and another high emission scenario, RCP 8.5, to forecast future climate change.

The snowmelt runoff model (SRM) was developed by Martinec in 1975 and designed for the simulation of climate change impacts on stream flow and water volume (Elias *et al.* 2016). Many studies have applied SRM by using MODIS snow-covered product for the simulation of daily discharge (Adnan *et al.* 2017; Jin *et al.* 2019; Khairul *et al.* 2019). SRM proved a successful model for the assessment of climate change impacts on runoff in the glacial-fed mountainous basins. The remote sensing observations are particularly valuable for providing detailed input of spatial data for SRM due to its spatial and temporal variability. SCAs derived from MODIS are frequently used for SRM due to its improved geolocation accuracy and spatial resolution as well as availability of snow (Mahmood *et al.* 2015).

Jhelum River has received less scientific research attention for monitoring climate change impacts on precipitation and snow cover variation due to the lack of a geographical and climatic database. The basin is a scarcely gauged mountainous basin due to its transboundary nature. Jhelum River is a part of the Himalaya mountains and UIB covering a variety of landforms and unique hydrology. As the Jhelum basin is part of the world's highest mountainous region the tops are covered with major glaciers. These glaciers are ultimately affected by climate change causing changes to the hydrology of the region. The Jhelum river has the second largest reservoir of the country, Mangla dam, for electricity generation to fulfill energy demands and irrigation purposes. The study was designed and investigated climatic and hydrologic changes' methodology in the presence of limited weather stations and a rugged topographical basin. The research used historical meteorological data along with Aphrodite data, GCMs, and MODIS to deal with the limitations of the available observed data. Modern technologies of downscaling SDSM and SRM were used to analyze the climate change impacts on runoff of the scarcely gauged Jhelum river basin.

STUDY AREA

The Jhelum river basin is part of the UIB and has two main tributaries, Neelum and Kunhar Rivers, that drain the southern slope of the Greater Himalayas and the northern slope of the Pir Punjal Mountains. Several studies have reported the South Asia region, including Himalayas and UIB, as a hot spot of climate change (Azmat *et al.* 2018). The upper Jhelum river basin is a transboundary region divided by the line of control between Pakistan and India. Jhelum basin covers a great altitudinal variation range from 235 to 6,063 m. Jhelum River is the second largest tributary of the Indus river system. The whole Jhelum basin drains into the Mangla Reservoir, the second largest reservoir of Pakistan, constructed in 1967. The Jhelum basin has a unique lithology and heterogeneous hydrology that make the basin susceptible to flooding. The geographical extent of the study area is between 73–75.7°E and 33–35.15°N (Figure 1).

MATERIALS

The historical daily data temperature and precipitation of eight weather stations were obtained from the Pakistan Meteorological Department (PMD) for the period of 1976–2018 (Table 1).

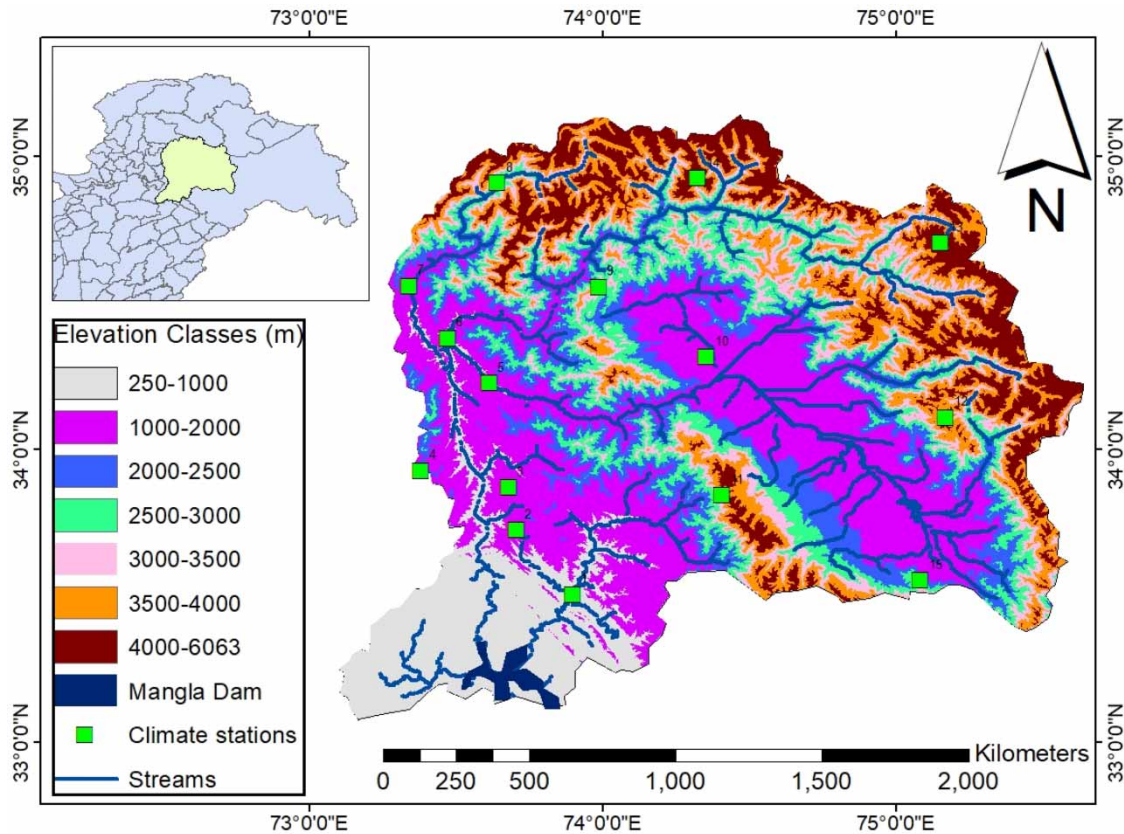


Figure 1 | Study area map with climate stations.

Table 1 | Basic information of weather stations in the Jhelum river basin

ID	Stations	Latitude (°N)	Longitude (°E)	Elevation (m) masl	Annual precipitation (mm)	Mean temperature (°C)
1	Kotli	33.50	73.90	614	1,255	22.2
2	Plandri	33.72	73.71	1,402	1,423	17.5
3	Rawalakot	33.87	73.68	1,676	1,346	16.26
4	Murree	33.91	73.38	2,213	1,780	12.86
5	Garidopatta	34.22	73.62	815	1,516	19.42
6	Muzaffarabad	34.37	73.48	702	1,388	20.64
7	Balakot	34.55	73.35	996	1,693	18.34
8	Naran	34.90	73.65	2,363	1,301	6.18

Table 1 describes the height variation of the weather stations in the region along with average precipitation and mean temperature. Kotli with a mean temperature of 22.2 °C and Naran with 6.18 °C are the hottest and coldest stations, respectively.

To overcome the issue of climatic stations' scarcity in the basin, Aphrodite data were coupled with stations' data. Aphrodite provides long-term daily gridded precipitation and temperature data sets for Asia downloaded from <https://climatedataguide.ucar.edu/> (NCAR Climate Data Guide n.d.).

Daily large-scale predictors expressing the current climatic condition (1961–2005) of NCEP (National Centers for Environmental Prediction) and the daily predictors for CCSM4 (RCP4.5 and RCP8.5) for 1961–2099 were downloaded from a Canadian website (<http://climate-scenarios.canada.ca/>; Canadian Climate Data and Scenarios n.d.).

A list of 26 NCEP predictors and CCSM4 predictors were processed to eliminate spatial differences for further use in the SDSM model. GCM from CMIP5 group CCSM4 data was selected due to its good correlation (0.9) with the baseline data set in the Indus river basin (Waheed 2015).

The global digital elevation model (GDEM) ASTER 30 m was used for zone classification of the study area.

MODIS product MOD10A2 of spatial resolution 500 m × 500 m was downloaded for the period of 2001–2018 from National Snow and Ice Data Center (NSIDC) (<https://nsidc.org/data/modis/>; MODIS data n.d.).

The measured daily discharge data for the Mangla hydrostation were acquired from Water and Power Development Authority–Surface Water Hydrology Project (WAPDA–SWHP).

METHODS

Statistical downscaling method (SDSM)

SDSM was used in combination with a stochastic weather generator (SWG) and multiple linear regression (MLR). NCEP and GCM predictors were applied by the SWG for the generation of daily time series (Mahmood *et al.* 2015). The success of statistical downscaling depends on the predictor variables' selection carried out using a combination of partial correlation, correlation matrix, and P value. The SDSM conditional sub-model was used for precipitation and for the temperature data. MLR was used to establish the relationship between observations (temperature and precipitation) as predicted variables and large-scale NCEP and CCSM4 predictors as independent variables by using SDSM. The best predictors selected based on the partial correlation results between predictors and predictands are shown in Table 2.

SDSM was calibrated for a period of 30 years (1976–2005) and validated for the period 2006–2015. The root mean square error (RMSE), coefficient of determination (R^2), correlation coefficient (R), absolute mean error (AME), and mean bias error (MBE) were calculated between observed points and predicted points for the validation period (2006–2015) as shown in Table 3.

The biases from the downscaled data were eliminated using mean based biased correction method (MB-BC) to remove any systematic errors in temperature and precipitation simulations during the downscaling process. MB-BC used differences between the mean of observed data and GCM simulation for the baseline period (Keteklahijani *et al.* 2019). Equations (1) and (2) are used for bias correction of temperature and precipitation data sets:

$$T_{de-biased} = T_{sim(2020-2099)} \times (T_{sim(1975-2005)} - T_{obs(1975-2005)}) \quad (1)$$

$$P_{de-biased} = P_{sim(2020-2099)} \times \left(\frac{P_{obs(1975-2005)}}{P_{sim(1975-2005)}} \right) \quad (2)$$

Table 2 | NCEP predictor variables

No.	Daily predictor variable description	Code	Absolute partial correlation coefficient (<i>abs. Pr.</i>)	
			Temperature	Precipitation
1	Mean sea level pressure	Mslp	–	0.14
2	500 hPa relative humidity	r500	0.28	0.13
3	850 hPa vorticity	P8_z	0.25	0.09
4	Surface zonal velocity	p_u	0.35	–
5	500 hPa vorticity	p5_z	0.15	0.10
6	Surface vorticity	p_z	0.31	–
7	500 hPa wind direction	p5th	0.29	0.11
8	850 hPa relative humidity	r850	0.30	0.13
9	Surface zonal velocity	p_u	0.41	–
10	850 hPa meridional velocity	p8_v	–	0.16
11	500 hPa meridional velocity	p5_v	–	0.22
12	Surface specific humidity	Shum	–	0.22
13	Mean temperature at 2 m	temp	0.75	–

Table 3 | Performance assessment of SDSM during validation period (2006–2015)

ID	Stations	R	R ²	RMSE	AME	MBE
1	Kotli	0.79	0.98	1.02	0.78	0.84
2	Plandri	0.88	0.87	0.8	0.71	0.85
3	Rawalakot	0.93	0.86	0.57	0.49	0.87
4	Murree	0.87	0.91	1.02	0.86	1.21
5	Garidopatta	0.86	0.82	0.92	0.78	0.94
6	Muzaffarabad	0.91	0.85	0.86	0.71	0.95
7	Balakot	0.89	0.92	0.77	0.49	0.97
8	Naran	0.83	0.89	1.01	0.86	1.2

where $T_{de-biased}$ and $P_{de-biased}$ denote biased corrected data for temperature and precipitation, respectively, for the future projected periods. T_{sim} and P_{sim} are the simulated downscaled data by SDSM and T_{obs} and P_{obs} are used for observed data.

Snowmelt runoff model (SRM)

SRM used characteristics of the basin and climatic variables that were distributed over the elevation zones of the basin to generate runoff. SRM was used for simulation and forecasting of the daily river flows by considering climate change effects on snow cover and runoff (Tahir *et al.* 2017). SRM is a comparatively simple hydrological model based on the degree day factor and considered remote sensing data for SCA as input variable (Jin *et al.* 2019). The SRM equation is as follows (Martinec *et al.* 1998):

$$Q_{n+1} = c_n[a_n(T_n + \Delta T_n)S_n + P_n]A \cdot \frac{10000}{86400} (1 - k_{n+1}) + Q_n k_{n+1} \quad (3)$$

where Q denotes the average daily discharge of the basin (m^3/s), c_{Rn} and c_{Sn} are the coefficient of rain and snow, respectively, a_n is the degree day factor, T_n is the number of degree days, ΔT_n is the adjustment by temperature lapse rate from the meteorological station to average hypsometric elevation of the zone ($^{\circ}C$ d), S_n is the percentage of SCA to the total area, P_n is the precipitation contributing to the runoff, A is the area of the elevation zone in km^2 , k is the recession coefficient indicating the decline in discharge for the period without snowmelt or rainfall, and n is the sequence of days during the discharge computation period. SRM used daily snow cover, precipitation, temperature, and basin characteristics as input variables and degree day factor, temperature lapse rate, runoff coefficient (for snow and rain), critical temperature, rainfall contributing area, recession coefficient, and time lag as parameters. T_{crit} ($^{\circ}C$) is critical temperature that differentiates precipitation into rain and snow. The critical temperature was identified using long-term temperature against rainfall or snow for the baseline climatic indicators (T and P). If $T < T_{crit}$ there is the chance for snowfall, and vice versa. Recession coefficient is the amount of the daily melt water that directly becomes part of the runoff and it also compensates the previous day's snowmelt contribution on a given day. The best way to determine k value is analysis of historical discharge data.

The temperature, precipitation, and SCA of each hypsometric zone considered three basic input variables for SRM. Basin characteristics such as latitude–longitude, number and area of zones, and mean hypsometric curve were used for discharge calculation. The Jhelum river basin was divided into elevation zones to generate the hypsometric curve (Table 4).

The generalized parameter values used for calibration of SRM were adjusted in each elevation zone according to zone characteristics with the help of published local literature (Adnan *et al.* 2017; Tahir *et al.* 2017) (Table 5). The default value of lag time 18 hr was used to compensate daily glacial and snow melt as well as rainfall contribution in each elevation zone. The runoff coefficient of snow and rainfall was used in the SRM to compensate for losses due to evapotranspiration, infiltration, etc.

SRM was calibrated for the time period of 2001–2018 to evaluate model efficiency evaluated by comparison between computed and measured discharge by volume difference (Dv%) and NSE by using the equations as follows (Tahir *et al.* 2017;

Table 4 | Catchment area under different elevation zones

Zone	Elevation class (masl)	Mean elevation (masl)	Area (km ²)	Area (%)
A	250–1,000	625	6,247	18
B	1,000–2,000	1,500	1,383	4
C	2,000–2,500	2,250	5,904	17
D	2,500–3,000	2,750	5,598	16
E	3,000–3,500	3,250	4,957	14
F	3,500–4,000	3,750	5,388	16
G	4,000–6,063	5,032	5,047	15

Table 5 | Calibration parameter values in the SRM

Parameter	Values	Parameter	Values
Temperature lapse rate (°C/100 m)	0.65	Rainfall contributing area (RCA)	0 (Sep–Jun), 1 (Jun–Aug)
T_{crit} (°C)	0	Reference elevation (m)	3,150
Degree day factor (cm °C ⁻¹ d ⁻¹)	0.3–0.7	Rainfall threshold (cm)	7.0
Lag time (hr)	18	Runoff coefficient for rain (c_{Rn})	0.07–0.58
Runoff coefficient for snow (c_{Sn})	0.02–0.35	Recession coefficient X_{coeff} , Y_{coeff}	0.7 (Apr–Sep), 1.09 (Oct–Mar) 0.02

Jin *et al.* 2019):

$$NSE = 1 - \frac{\sum_{i=1}^n (Q_i - Q'_i)^2}{\sum_{i=1}^n (Q_i - \bar{Q})^2} \quad (4)$$

$$D_v = \frac{VR - VR'}{VR} \times 100 \quad (5)$$

where Q_i is the measured discharge during the simulated period, Q'_i is the simulated discharge, n is the number of simulated days. VR is the measured runoff volume while VR' is the simulated runoff. The simulated and measured discharge for the time period of 2001–2018 was plotted using hydrographs. The de-biased downscaled climatic data were used as SRM input to simulate future discharge for the 21st century under both scenarios. The hydrographs for RCP4.5 and RCP8.5 were drawn to analyze the future water availability for the 21st century of the Jhelum river basin.

RESULTS AND DISCUSSION

Climatic changes

SDSM showed better performance for temperature as compared to precipitation because downscaling of precipitation is a conditional process and dependent on other processes such as cloud cover, humidity, and wet days (Hassan *et al.* 2014). Overall, all indicators depicted the same trend of error for temperature and precipitation, but determination of coefficient (R^2) results are more acceptable for both temperature and precipitation. After calibration and validation of SDSM, simulated de-biased data of precipitation and temperature for the period of 2020–2099 were divided into four periods, i.e., 2030s (2020–2040), 2050s (2041–2060), 2070s (2061–2080), and 2090s (2081–2099) for spatial analysis. The final outputs of projections were compared with the baseline period data to get a clear picture of future climate changes (Huang *et al.* 2011; Mahmood *et al.* 2015). The downscaled data were interpolated using the kriging method (Figures 2 and 3).

Spatial projections of mean annual temperature depicted an increasing trend in the north (more elevated region) as compared to the southwest (low lying area) of the basin, for both RCPs. The altitudinal variation dominated the temperature changes of the basin as major changes in temperature were observed in elevated mountainous zones as compared to low

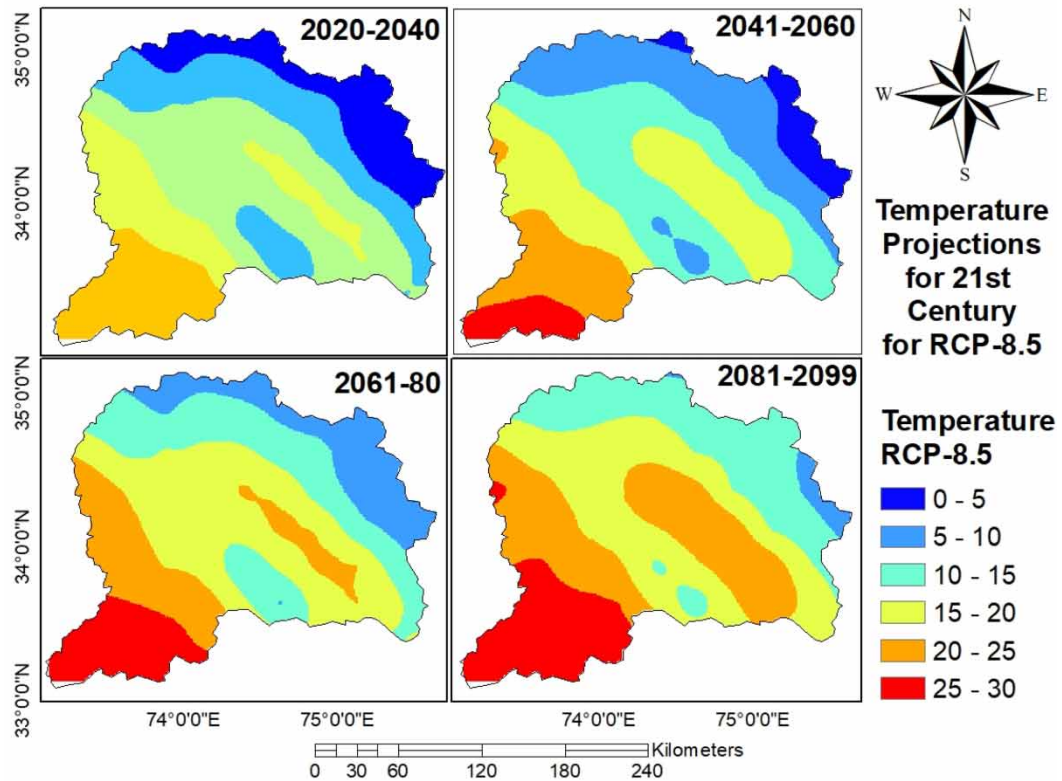
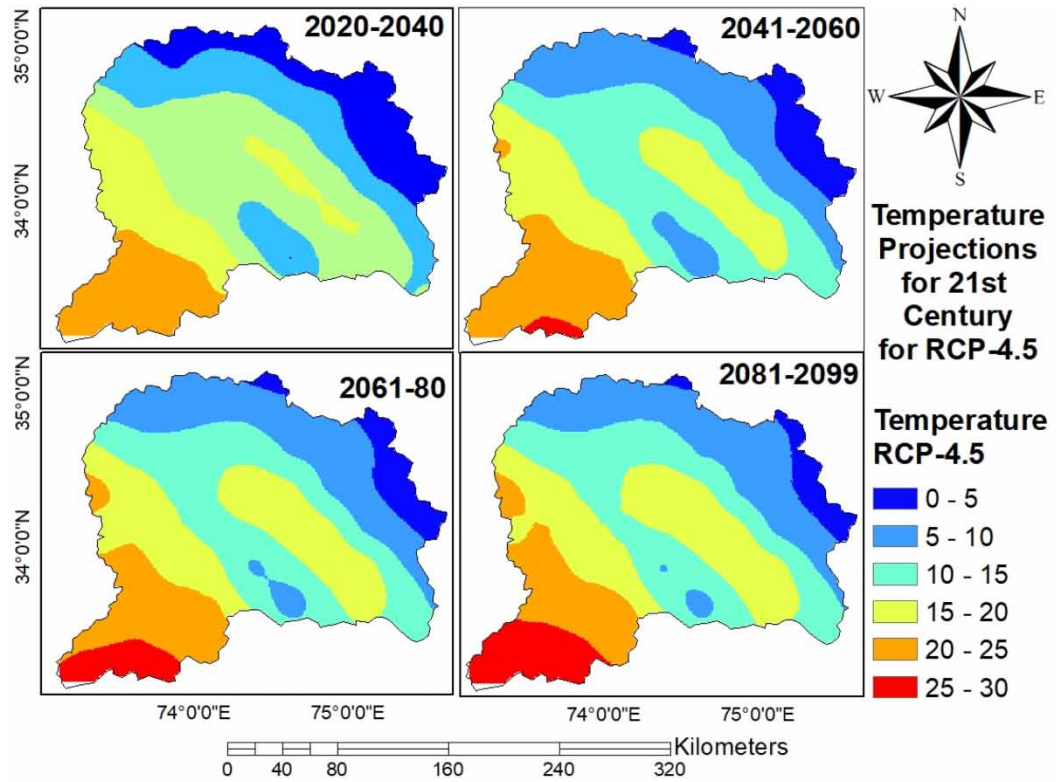


Figure 2 | Spatial distribution for mean annual temperature (°C) for RCP4.5 and 8.5 scenarios.

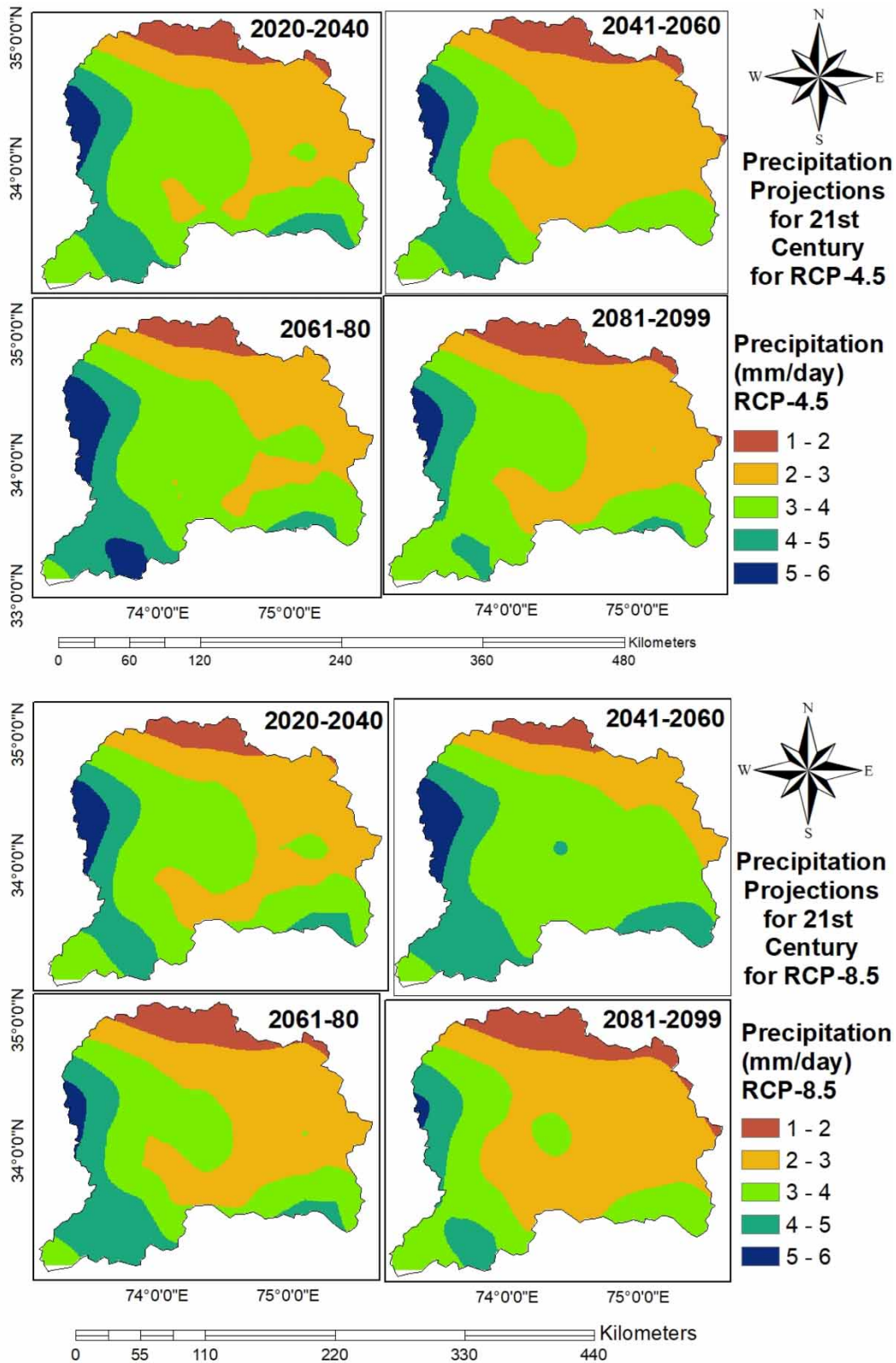


Figure 3 | Spatial distribution for mean annual precipitation for RCP4.5 and 8.5 scenarios.

lying areas and that these mountainous regions are more susceptible to rising temperature during the coming decades was also supported by other studies (Abbasnia & Toros 2016). The temperature changes of 1.2 °C were observed for the 2030s and 2.7 °C for the 2090s, and 2.2 °C for the 2030s and 5.6 °C for the 2090s for RCP4.5 and RCP8.5, respectively. Overall, Jhelum basin depicted a rising trend in temperature from the 2030s to 2090s for both scenarios.

Precipitation projections in comparison to the baseline period predicted a slight increase under both scenarios until the end of the century. The zones shifted from the highly precipitated area to the lower which is more dominant under RCP8.5 projection as compared to RCP4.5 showing an intensity of pattern. The precipitation projections from the 2030s to the 2090s depicted an increasing precipitation trend in the western part and decline in the eastern part of the basin that may be due to the monsoon pattern. The precipitation increased by 3.89% for the 2030s and 5.6% for 2090s and 5.4% for the 2030s and 7.1% for the 2090s for RCP4.5 and RCP8.5, respectively. The increasing trend of temperature change observed from the 2030s to 2090s is more significant and clear as compared to the precipitation pattern in the basin. Overall temperature is a consistent variable as compared to precipitation but both variables show increasing trend over time. RCP4.5 depicts a gentle rise in temperature in contrast with RCP8.5, depicting the story line for both scenarios. The increase in average temperature is 1.5 °C and 3.8 °C, and increase in mean annual precipitation is about 2–7% for the 21st century as compared to the baseline period for the Jhelum river basin.

Hydrological changes

The SRM model was calibrated using variables (temperature, precipitation, and SCA) and parameters (Table 5). The results of the SRM calibration depicted that recession coefficient (k) and runoff coefficient for snow (c_{sn}) were found to be the sensitive parameters. The climatic variables (temperature and precipitation) play an important role in runoff calculation by SRM and Aphrodite data that proved useful for the scarcely gauged mountainous basin. The zones D, E, F, G (2,500–6,063 m) covered the major proportion of the basin contributing snowmelt runoff production. The statistical parameters volume difference ($Dv^0\%$) and NSE indicated a satisfactory application of the SRM over the Jhelum river basin, as presented in Table 6.

The results of NSE and $Dv^0\%$ varied between 0.78–0.98 and –2.96–4.58, respectively, indicating the effectiveness of the SRM calibration for the Jhelum river basin. The year-wise simulated and observed discharge was compared for the period of 2001–2018 (Figure 4).

The results of simulated discharge showed an overestimation of discharge for the summer months. This may be due to the contribution of monsoon along with snow melting because SRM is less sensitive to precipitation and more sensitive to the SCA and temperature (Azmat *et al.* 2018). The de-biased corrected downscaled data of temperature and precipitation used in the SRM to predict future discharge for the 21st century for RCP4.5 and RCP8.5 is shown in Figure 5.

The results suggested that runoff of Jhelum river continuously increased over time but the increasing trend of river flow is more prominent, 5.5% and 8.6% during the first two time slices (2020–2040 and 2041–2060), respectively, whereas during the last two slices (2061–2080 and 2081–2099) discharge reduced to 3% and 7.1%, respectively. The rise in average annual temperature may cause an increase in river flow for RCP4.5 and RCP8.5 until the end of the century. In the latter half of the century the river flow showed a decline that may be due to temperature changes (1.5 °C and 3.8 °C for RCP4.5 and

Table 6 | Accuracy assessment of the SRM

Years	Volume difference (Dv %)	NSE	Years	Volume difference (Dv %)	NSE
2001	–2.96	0.78	2010	–1.82	0.85
2002	1.69	0.82	2011	–1.91	0.86
2003	–1.42	0.9	2012	0.81	0.9
2004	1.97	0.91	2013	–0.60	0.96
2005	1.77	0.93	2014	1.48	0.82
2006	–2.61	0.85	2015	–0.65	0.97
2007	2.27	0.8	2016	0.84	0.91
2008	–1.80	0.86	2017	–1.51	0.92
2009	1.45	0.84	2018	4.58	0.89

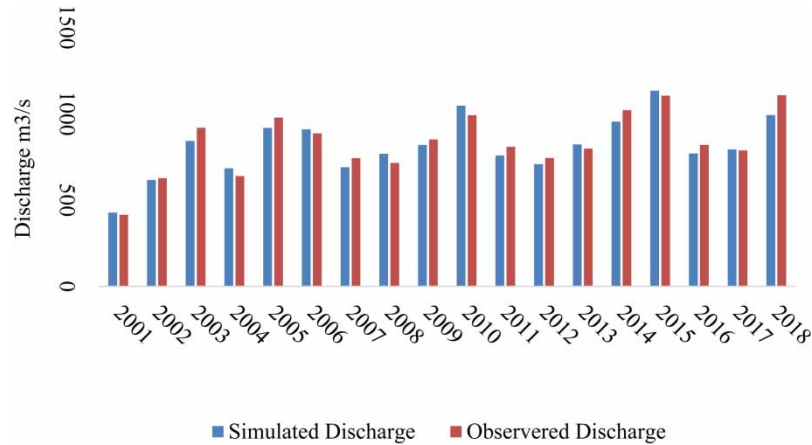


Figure 4 | Comparison of simulated and measured discharge for 2001–2018.

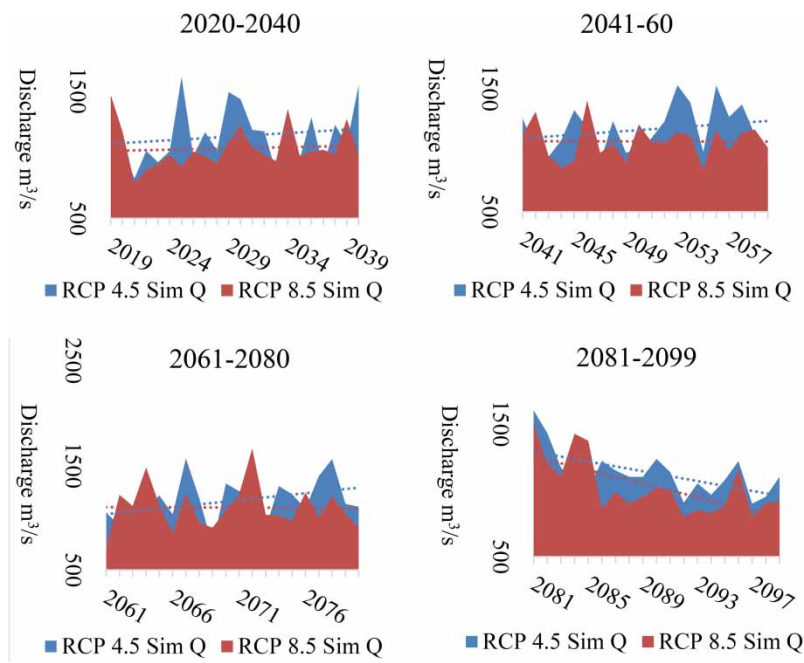


Figure 5 | Simulated discharge for 2020–2100 for RCP4.5 and RCP8.5.

RCP8.5) causing a reduction in glacial mass until the end of the 21st century. Overall increase in surface runoff of about 3.3–7.4% was projected until the end of the 21st century as compared to the baseline period. The results of SDSM and SRM simulations are in line with various previous studies that suggested a substantial increase in precipitation and temperature which causes an increase in runoff over the Jhelum river basin (Azmat *et al.* 2018).

The climatic and hydrological changes indicated continuous increase in precipitation and temperature over the Jhelum river basin. The temperature is the more crucial variable to affect precipitation, snow, and glaciers for the hydrological cycle. The situation of temperature rise (with considerable variation in precipitation) may inflate the summer flows but could be critical for the permanent snow and glacial reserves in the Jhelum river basin. This increase in river flow may be beneficial for hydroelectric power and irrigation if the situation is mitigated properly through dam and reservoir construction; otherwise, without adopting water management options, it might be a curse in terms of flood hazard in the low-lying areas. Flooding has already affected available larger-capacity Pakistan dams (Tarbela and Mangla) by silt accumulation and they are unable to provide storage and hydroelectric power according to the requirements (Latif *et al.* 2019). The study results predict

severe climatic and hydrological changes for the 21st century in the mountainous Jhelum river basin. Thus, it would be necessary to construct large-capacity reservoirs, keeping in view the issues of water demand and flood protection due to climate change.

CONCLUSIONS

The study examined the climatic and hydrologic changes using SDSM and SRM with good accuracy assessment although these projections are a challenge for the transboundary scarcely gauged mountainous Jhelum river basin. The conclusions drawn from the results obtained in the study are as follows:

- The Jhelum river basin has a limited number of weather stations due to its rugged topography and transboundary nature. The study was designed to cope with the issue of scarce weather observation data by coupling this with Aphrodite data. The SDSM technique is a modern statistical technique to bridge the relationship between the coarse grid GCM data and local weather data and used to predict local climate of the basin for the 21st century. RCPs are the new GHG concentration-based scenarios that help to predict the future climatic indicators of the region. Climatic projections were further used in the SRM to predict future hydrological changes in the basin. The study first investigated the climatic changes in detail by using the downscaling technique, then projected the hydrological changes to cope with the future water availability issues of the basin by drawing hydrographs for the 21st century.
- Although Aphrodite data used along with observed meteorological data helped to improve the accuracy of SDSM and SRM in the scarcely gauged mountainous basin, more weather stations should be installed in this highly elevated glacial region.
- The SDSM unconditional sub-model used for temperature proved to be more efficient than the SDSM conditional model for precipitation.
- SDSM results indicated that temperature and precipitation changes become more robust in the latter half of the century as compared to the first half of the century.
- SRM hydrologic projections are based on the climatic projections of temperature and precipitation so the accuracy assessment of SDSM is crucial to predict hydrological changes.
- SRM model parameters can be changed on a seasonal basin to get more accurate results of discharge.
- The study focused on the SDSM and SRM model to assess the climatic and hydrological changes at the local basin level. The downscaling and the runoff calculation made the work extensive so that is why only GCM CCSM4 data were used for the projections. However, multiple GCMs can be used to compare the results for the climatic and hydrologic changes for the 21st century in the Jhelum river basin.
- The Jhelum river basin is part of the Indus basin fed by the Himalaya mountains which have the most major glaciers in the world after the polar regions and are more susceptible to climate change due to an increase in temperature. The basin requires attention for better management for water scarcity and flooding issues for the 21st century by building dams and adapting water conservation strategies.

ACKNOWLEDGEMENTS

The authors would like to acknowledge Pakistan Meteorological Department (PMD) and Water and Power Development Authority (WAPDA) for meteorological and hydrological data. We would like to acknowledge Canadian climate center and National snow and ice data center for free data sets. We would like to acknowledge National Agriculture Research Council (NARC, Pakistan) for the ASTER GDEM (30 m) data. The author would like to thank the University of Gujrat for financial support and PMAS arid agriculture university, Rawalpindi for accommodating me to carryout doctoral research.

DATA AVAILABILITY STATEMENT

All relevant data are available from an online repository or repositories (<https://climatedataguide.ucar.edu/>; (<https://climate-scenarios.canada.ca/?page=main>).

REFERENCES

- Abbasnia, M. & Toros, H. 2016 Future changes in maximum temperature using the statistical downscaling model (SDSM) at selected stations of Iran. *Modeling Earth Systems and Environment* 2 (2). <https://doi.org/10.1007/s40808-016-0112-z>.

- Adnan, M., Nabi, G., Kang, S., Zhang, G., Adnan, R. M., Anjum, M. N., Iqbal, M. & Ali, A. F. 2017 Snowmelt runoff modelling under projected climate change patterns in the Gilgit river basin of northern Pakistan. *Polish Journal of Environmental Studies* **26** (2), 525–542. <https://doi.org/10.15244/pjoes/66719>.
- Azmat, M., Qamar, M. U., Huggel, C. & Hussain, E. 2018 Future climate and cryosphere impacts on the hydrology of a scarcely gauged catchment on the Jhelum river basin, Northern Pakistan. *Science of the Total Environment* **639**, 961–976. <https://doi.org/10.1016/j.scitotenv.2018.05.206>.
- Baek, H. J., Lee, J., Lee, H. S., Hyun, Y. K., Cho, C., Kwon, W. T., Marzin, C., Gan, S. Y., Kim, M. J., Choi, D. H., Lee, J., Lee, J., Boo, K. O., Kang, H. S. & Byun, Y. H. 2013 Climate change in the 21st century simulated by HadGEM2-AO under representative concentration pathways. *Asia-Pacific Journal of Atmospheric Sciences* **49** (5), 603–618. <https://doi.org/10.1007/s13143-013-0053-7>.
- Canadian Climate Data and Scenarios n.d. Available from: <http://climate-scenarios.canada.ca/?page = main> (accessed 15 July 2018).
- Elias, E., Rango, A., Steele, C. M., Mejia, J. F., Baca, R., James, D., Schrader, S. & Gronemeyer, P. 2016 Simulated impact of climate change on hydrology of multiple watersheds using traditional and recommended snowmelt runoff model methodology. *Journal of Water and Climate Change* **7** (4), 665–682. <https://doi.org/10.2166/wcc.2016.097>.
- Hasan, D. S. N. A. P. A., Ratnayake, U., Shams, S., Nayan, Z. B. H. & Rahman, E. K. A. 2018 Prediction of climate change in Brunei Darussalam using statistical downscaling model. *Theoretical and Applied Climatology* **133** (1–2), 343–360. <https://doi.org/10.1007/s00704-017-2172-z>.
- Hassan, Z., Shamsudin, S. & Harun, S. 2014 Application of SDSM and LARS-WG for simulating and downscaling of rainfall and temperature. *Theoretical and Applied Climatology* **116** (1–2), 243–257. <https://doi.org/10.1007/s00704-013-0951-8>.
- Huang, J., Zhang, J., Zhang, Z., Xu, C. Y., Wang, B. & Yao, J. 2011 Estimation of future precipitation change in the Yangtze River basin by using statistical downscaling method. *Stochastic Environmental Research and Risk Assessment* **25** (6), 781–792. <https://doi.org/10.1007/s00477-010-0441-9>.
- IPCC 2013 IPCC Technical summary. In: *Climate Change 2013: The Physical Science Basis. Contribution of Working Group I to the Fifth Assessment Report of the Intergovernmental Panel on Climate Change*.
- Jin, H., Ju, Q., Yu, Z., Hao, J., Gu, H., Gu, H. & Li, W. 2019 Simulation of snowmelt runoff and sensitivity analysis in the Nyang River Basin, southeastern Qinghai-Tibetan Plateau, China. *Natural Hazards* **99**, 931–950. <https://doi.org/10.1007/s11069-019-03784-0>.
- Keteklahijani, V. K., Alimohammadi, S. & Fattahi, E. 2019 Predicting changes in monthly streamflow to Karaj dam reservoir, Iran, in climate change condition and assessing its uncertainty. *Ain Shams Engineering Journal* **10** (4), 669–679. <https://doi.org/10.1016/j.asej.2018.11.004>.
- Khairul, M., Shamsuddin, N., Nor, W., Sulaiman, A., Ramli, M. F., Kusin, F. M. & Sefie, A. 2019 Advances in sustainable and environmental hydrology, hydrogeology, hydrochemistry and water resources. In: *Proceedings of the 1st Springer Conference of the Arabian Journal of Geosciences*. Springer International Publishing. <https://doi.org/10.1007/978-3-030-01572-5>.
- Latif, Y., Ma, Y., Ma, W., Sher, M. & Muhammad, Y. 2019 Snowmelt runoff simulation during early 21st century using hydrological modelling in the Snow-Fed Terrain of Gilgit River Basin (Pakistan). In: *Conference of the Arabian Journal of Geosciences*. pp. 73–76. https://doi.org/https://doi.org/10.1007/978-3-030-01572-5_18.
- Mahmood, R. & Jia, S. 2016 Assessment of impacts of climate change on the water resources of the transboundary Jhelum River Basin of Pakistan and India. *Water (Switzerland)* **8** (6). <https://doi.org/10.3390/W8060246>.
- Mahmood, R., Babel, M. S. & Jia, S. 2015 Assessment of temporal and spatial changes of future climate in the Jhelum river basin, Pakistan and India. *Weather and Climate Extremes* **10**, 40–55. <https://doi.org/10.1016/j.wace.2015.07.002>.
- Mandal, S., Breach, P. A. & Simonovic, S. P. 2016 Uncertainty in precipitation projection under changing climate conditions: a regional case study. *American Journal of Climate Change* **5** (01), 116–132. <https://doi.org/10.4236/ajcc.2016.51012>.
- Martinec, J., Rango, A. & Roberts, R. 1998 *Snowmelt Runoff Model (SRM) User's Manual (Updated Edition 1998)*. p. 177.
- MODIS data n.d. Available from: https://nsidc.org/data/modis/order_data.html (accessed 18 October 2018).
- NCAR Climate Data Guide n.d. Available from: <https://climatedataguide.ucar.edu/climate-data/aphrodite-asian-precipitation-highly-resolved-observational-data-integration-towards> (accessed 20 October 2017).
- Pervez, M. S. & Henebry, G. M. 2014 Projections of the Ganges-Brahmaputra precipitation-downscaled from GCM predictors. *Journal of Hydrology* **517**, 120–134. <https://doi.org/10.1016/j.jhydrol.2014.05.016>.
- Tahir, A. A., Hakeem, S. A., Hu, T., Hayat, H. & Yasir, M. 2017 Simulation of snowmelt-runoff under climate change scenarios in a data-scarce mountain environment. *International Journal of Digital Earth* **12** (8), 910–930. <https://doi.org/10.1080/17538947.2017.1371254>.
- Tahir, T., Hashim, A. M. & Yusof, K. W. 2018 Statistical downscaling of rainfall under transitional climate in Limbang River Basin by using SDSM. *IOP Conference Series: Earth and Environmental Science* **140** (1). <https://doi.org/10.1088/1755-1315/140/1/012037>.
- Waheed, I. B. A. 2015 Generation of high-resolution gridded climate fields for the Upper Indus River Basin by downscaling CMIP5 outputs. *Journal of Earth Science & Climatic Change* **6** (02). <https://doi.org/10.4172/2157-7617.1000254>.

First received 25 September 2020; accepted in revised form 10 August 2021. Available online 9 September 2021